# Effective Evaluation of Catalytic Deoxygenation for *in situ* Catalytic Fast Pyrolysis using Gas Chromatography-High Resolution Mass Spectrometry

D. Paul Cole and Young Jin Lee*

Department of Chemistry, Iowa State University, Ames, IA 50011, USA

* To whom correspondence should be addressed. E-mail: yjlee@iastate.edu

**ABSTRACT**

Effective deoxygenation in catalytic fast pyrolysis (CFP) is crucial for bio-oil stabilization and its successful commercialization. Herein, we utilize a new analytical platform that couples gas chromatography (GC) to dopant-assisted atmospheric pressure chemical ionization (dAPCI) time-of-flight mass spectrometry (TOF MS) to evaluate catalytic deoxygenation of cellulose pyrolysis. Soft ionization and accurate mass measurement through dAPCI-TOF MS allows direct chemical composition analysis of GC-separated molecules, regardless of their presence in the database. The analytical approach was successfully demonstrated for its ability to evaluate catalytic efficiency of different catalysts and to monitor the change in CFP reaction products with catalyst-to-biomass load ratio. A total of 142 compounds could be analyzed with this approach compared to 38 compounds in traditional Py-GC-EI-MS analysis.

***Keywords:*** Cellulose pyrolysis, dopant-assisted APCI, catalytic fast pyrolysis, zeolite, deoxygenation, bio-oil

## 1. Introduction

Fast pyrolysis of biomass has shown promise toward producing biofuel for transportation needs [1]. The feedstock is rapidly heated in the absence of oxygen to convert lignocellulosic biomass to a high yielding liquid product called bio-oil. Bio-oil is chemically distinct from crude oils due to its high oxygen content. Because of its incompatibility with the existing infrastructure, upgrading is necessary prior to processing with conventional petroleum oil refinery [2,3]. Particularly important is an efficient deoxygenation or hydrodeoxygenation process with minimal carbon loss. It is shown that complete deoxygenation can be achieved through catalytic upgrading; however, bio-crude yield is often reduced as more oxygen is removed. This is because the deoxygenation is typically accomplished by CO or $CO_2$ removal through decarbonylation or decarboxylation [2,4]. Coke formation within the catalysts pore is another source of significant carbon loss [2,5]. Therefore, catalytic upgrading should be developed to maximize carbon yield and minimize oxygen content.

Catalytic fast pyrolysis (CFP), either *in situ* within the pyrolysis reactor or *ex situ* immediately after pyrolysis, upgrades bio-oil vapor before quenching as liquid products and minimizes secondary reactions or bio-oil aging compared to the liquid product upgrading [6]. *Ex situ* CFP has several advantages over *in situ* CFP. It can independently control catalytic reaction conditions and generally has less coke formation. Furthermore, *in situ* CFP is not currently applicable to a commercial scale reactor due to the need of frequent exchange and/or regeneration of catalysts. However, because of its simplicity and minimal modification to existing reactors, *in situ* CFP is commonly used for lab scale demonstrations and studying catalytic reactions. The production of fully deoxygenated aromatic compounds, *e.g.* benzene, toluene, and xylenes (BTX), was demonstrated via *in situ* CFP [7]. CFP conversion of biomass

has been extensively studied with zeolite catalysts [8-12]. For example, Foster *et al.* studied optimum silica-to-alumina ratio for ZSM-5 catalyst to maximize aromatic yield and minimize char formation [12].

Characterization of CFP products is crucial to understand the catalytic reactions and develop efficient deoxygenation processes. Gas chromatography-mass spectrometry (GC-MS) is most commonly used to characterize CFP products because of its high-resolution separation capability and large mass spectral database. Micropyrolyzer is often attached to GC-MS and a small quantity of biomass material is loaded after premixing with catalysts for *in situ* CFP product analysis [13]. Electron ionization (EI) is typically employed to ionize molecules for MS analysis. EI is non-selective and highly energetic, and produces significant fragmentations that can be used to search the database for identification. However, it is not as useful for those compounds that are absent in the database or have no molecular ion peak due to significant fragmentation, which is often the case for many bio-oil compounds.

Various soft ionization techniques have been developed to minimize fragmentations, such as chemical ionization (CI), field ionization (FI), vacuum UV photoionization (VUV PI) with or without infrared laser desorption (IR LD), and laser-ablation resonance-enhanced multiphoton ionization (LA-REMPI) [14-19]. Atmospheric pressure chemical ionization (APCI), originally developed for GC-MS several decades ago, has been recently re-introduced after successful commercialization for LC-MS instrumentation [20-23]. It has an additional advantage of utilizing high-resolution mass spectrometers developed for LC-MS in GC-MS applications [24]. However, APCI still produces significant fragmentations for volatile small molecules, which limits its application for bio-oil analysis with GC-APCI-MS. Dopant-assisted APCI (dAPCI) has been developed and utilized for LC-MS to reduce fragmentations and increase ionization

efficiency [25,26], but has not been demonstrated for GC-MS.

Here, we developed dAPCI for GC-MS with ammonia as a dopant gas and applied to *in situ* CFP product analysis. In particular, a high-resolution time-of-flight mass spectrometer (TOF MS) is utilized for mass spectral data acquisition to directly determine the chemical compositions of CFP products. Cellulose was used in this study with ZSM-5 and zeolite Y (ZY) catalysts. Catalytic deoxygenation efficiency in the *in situ* CFP of cellulose pyrolysis was successfully evaluated with the new GC-dAPCI-TOF MS approach.

## 2. Materials and Methods

### 2.1. Materials

Sigmacell Cellulose Type 20 (20 µm particle size) and zeolite Y catalyst (Si/Al = 3; BET surface area of 948 $m^2$ $g^{-1}$) were purchased from Sigma-Aldrich (St. Louis, MO, USA). The ZSM-5 catalyst (Si/Al = 23; BET surface area of 425 $m^2$ $g^{-1}$) was obtained from Alfa Aesar (Ward Hill, MA, USA). Both catalysts were calcined in ambient air at 550˚C for 6 h inside an oven to convert from ammonium to proton form prior to use.

### 2.2. Pyrolysis – GC-TOF MS experiments

Pyrolysis studies were carried out using a drop-tube microfurnace pyrolyzer (Frontier Laboratories 3030S Micropyrolyzer, Fukushima, Japan) installed onto an Agilent 7890A gas chromatograph (Palo Alto, CA, USA). The GC is coupled with an Agilent 6200 time-of-flight mass spectrometer through an Agilent G3212 APCI interface. The GC separation was performed using a fused silica DB-1701 column (30 m x 0.25 mm i.d. x 0.25 µm). The oven temperature was programmed at an initial temperature of 35˚C for 5 min, ramped at 4˚C $min^{-1}$ to a final

temperature of 260˚C, and held for 5 min. Ultrahigh purity helium gas was used as a carrier gas with a flow rate of 100 mL $min^{-1}$ through the pyrolyzer. The gas flow was split 100:1 at the GC inlet resulting in a column flow rate of 1 mL $min^{-1}$. High purity ammonia gas (500 ppm in He; Praxair, Dansbury, CT, USA) was introduced into the APCI chamber at a flow rate of 1 ml $min^{-1}$ through a zero-dead volume tee that was installed in the GC oven. The pyrolyzer inlet, GC inlet, and GC/APCI transfer tube interfaces were set to 280˚C. APCI was operated at a corona discharge of 1 kV and the MS inlet was heated to 325˚C with a drying gas flow of 5 L $min^{-1}$. TOF MS has a scan speed faster than 1 ms per microscan for a mass range of *m/z* 60-1000, but averaged and saved every second.

Catalyst effectiveness during CFP was studied at different catalyst-to-cellulose load ratios (0:1, 1:1, 5:1, 10:1 by weight). A total of 500 µg of premixed cellulose and catalyst mixture were exactly weighed into sample cups prior to dropping into the microfurnace set at a pyrolysis temperature of 500˚C. For semi-quantitative analysis, extracted ion chromatograms (EIC) were generated in MassHunter Qualitative Data Analysis software (Agilent) based on the exact mass of each compound of interest, and integrated over the corresponding EIC peaks at the given retention time. Integrated EIC peak area values were exported to Excel and normalized on a per 100 µg cellulose basis. All the chemical compositions assigned in Table S1 are not present in a blank measurement and have signals greater than 0.1% relative abundance of the base peak, which is more than 6 times the base line noise.

For comparison, pyrolysis-GC-EI-MS analysis was performed for cellulose and a 1:1 mixture of ZSM-5:cellulose using Agilent 5975C MSD operated in EI mode with scanning *m/z* range of 35-650. All other conditions are exactly the same including pyrolysis conditions and GC column and programing. AMDIS software (NIST, v2.71, Build 134.27) was used for

analysis of Py-GC-EI-MS data for automatic deconvolution and database search. The NIST EI-MS spectral library (v2.0 g, 2011) was used with a minimum match score of 750.

## 3. Results and Discussion

### 3.1. Dopant-assisted APCI for GC-TOF MS

We have developed dopant-assisted APCI for GC-MS. Fig. 1 shows the schematic diagram of this instrumentation and illustrates the dAPCI region. A micropyrolyzer is directly attached to a GC for pyrolysis-GC-MS (Py-GC-MS) analysis. Time-of-flight mass spectrometer is used for mass spectrometric measurements, which is essential due to its high mass resolution (R = 12,500 at *m/z* 600). Unlike typical GC-MS, where electron ionization (EI) is used for fragmentation and database search, we softly ionize the molecules with dAPCI and directly determine the chemical compositions of molecules from the accurate mass information.

For dAPCI, pre-heated ammonia gas (500 ppm in helium) is fed through a tee inside the GC oven, flowing outside the GC column, and introduced to APCI interface as a sheath gas (inset diagram of Fig. 1). APCI corona discharge region is dominated by ammonia gas, predominantly ionizing ammonia to form ammonium cation, which then ionizes analyte molecules via protonation or ammonium adduct formation. Because analytes are indirectly ionized, as in CI, it is much softer than APCI without dopant gas. Furthermore, any extra internal energy during protonation or ammonium adduct formation (*e.g.*, proton affinity difference between analytes and ammonia in case of protonation) is rapidly cooled down through millions of collisions with atmospheric molecules before they are injected into the mass spectrometer; thus, dAPCI produces almost no fragmentation. In typical CI occurring inside vacuum, there is no sufficient collisional cooling and extra internal energy leads to significant fragmentations.

Fig. 2 shows levoglucosan mass spectra with and without ammonia dopant gas. Without dopant, levoglucosan is detected as a protonated ion with significant fragmentation of one or two water loss(es). However, with ammonia, there is almost no fragmentation and levoglucosan is detected as an ammonium adduct with 20 times signal improvement. It is in contrast to EI where levoglucosan or other carbohydrate molecules are completely broken apart and no molecular ion can be observed. Overall, wide classes of compounds are ionized by dAPCI with no or minimal fragmentations; multi-oxygenated compounds (*e.g.* furans, anhydrosugars) are mostly ionized as an ammonium adduct, phenolic compounds produced in lignin pyrolysis are mostly ionized as a protonated form, and aromatic hydrocarbons are ionized as a radical ion form.

Our newly developed dAPCI method is especially useful when connected to a TOF MS and applied to complex unknown analysis such as in Py-GC-MS. Many of the compounds in Py-GC-MS are not in the database (see section 3.2 and Table S1) and the information available through conventional GC-EI-MS is very limited. On the other hand, TOF MS combined with dAPCI can softly ionize the compounds with no or minimal fragmentation and directly determine their chemical compositions. The dAPCI-TOF MS also provides excellent sensitivity (detection limit of ten femtomole level) and dynamic range of up to five orders of magnitude. Lack of structural information and unavailability of database search are the current limitations but the chemical compositions of the pyrolysis or upgraded products provide sufficient information for the purpose of catalytic deoxygenation monitoring, as demonstrated here.

Our ability to directly determine all the chemical compositions leads to the realization that many of the compounds in Table S1 are actually structural isomers. For example, we observed five structural isomers of $C_6H_{10}O_5$ and nineteen structural isomers of $C_6H_8O_4$. This is in contrast to only two known structural isomers in Py-GC-EI-MS analysis for both the chemical

compositions. For $C_6H_{10}O_5$, 1,6-anhydro-β-D-glucopyranose (levoglucosan) and 1,6-anhydro-β-D-glucofuranose are reported [32]. For $C_6H_8O_4$, 1,5-anhydro-4-deoxy-D-glycerohex-1-en-3-ulose and 1,4;3,6-dianhydro-α-D-glucopyranose (DAGP) are previously reported [31]. It is not surprising many more structural isomers are present than previously reported. When a glycosidic bond is cleaved in cellulose chain, several different structural isomers are possible depending upon where and how the broken bond is re-arranged to form stable compounds. Levoglucosan is most stable and produced in high yield, thus known for a long time, but thermodynamics allows some other structural isomers possible at high temperature of 500˚C. Although many of them have not been fully characterized due to their low abundances, we could at least confirm their presence after GC separation followed by high-resolution mass spectrometric analysis. In case of $C_6H_8O_4$, many more structural isomers would be possible depending on where water loss occurs in several structural isomers of $C_6H_{10}O_5$, among which we found a total of nineteen isomers.

### 3.2. Py-GC-dAPCI-TOF MS analysis for *in situ* catalytic fast pyrolysis

Py-GC-dAPCI-TOF MS analysis was performed for cellulose pyrolysis with and without catalysts. Fig. 3 shows base peak chromatograms (BPCs) for fast pyrolysis of cellulose and catalyst-cellulose mixtures at 5:1 ratio with ZY and ZSM-5. Major peaks are labeled with their corresponding heteroatom classes. Characterization and identification of cellulose pyrolysis products is previously reported, but only for major compounds [27-31]. The most abundant compound in cellulose pyrolysis is levoglucosan ($C_6H_{10}O_5$) having a retention time of 44.4 min, followed by glycolaldehyde ($C_2H_4O_2$) at 5.5 min and 5-hydroxymethylfurfural ($C_6H_6O_3$) at 34.6 min. The overall chromatogram pattern and ion abundances are relatively in good agreement

with other reported data [32,33], except that very low mass compounds are missing such as formic acid. Formic acid has *m/z* 64 as an ammonium adduct, which is close to the low mass cutoff of the current instrumentation, *m/z* 60, and significant mass discrimination is expected. Additionally, very volatile compounds seem to have low efficiency with the current instrumentation.

*In situ* CFP with zeolite catalysts (Fig. 3B and 3C) show distinct differences compared to the control (Fig. 3A). With ZY catalyst (Fig. 3B), ion signals for highly oxygenated compounds are decreased (note y-scale is ten times different between Fig. 3A and 3B) and converted to various low oxygen compounds, making the chromatogram very complex. In case of ZSM-5 (Fig. 3C), highly oxygenated compounds are mostly gone and $O_1$ and fully deoxygenated hydrocarbon compounds (HC) dominate the chromatogram. This is in good agreement with the previous report that ZSM-5 is very efficient in deoxygenation [12]. This effect is most noticeable through the presence of highly abundant aromatic hydrocarbons (*e.g.*, those peaks at the retention time of 26.9, 30.7, 46.1, and 49.0 min for naphthalene, methylnaphthalene, anthracene, and methylnaphthalene, respectively), and the decrease in levoglucosan ion intensity by one hundred times. The difference between ZSM-5 and ZY can be attributed to zeolite pore structure and acidity. ZSM-5 has smaller pores and greater acidity (straight 10 member-ring, 5.4 Å) compared to ZY (circular 12 member-rings, 7.4 Å) [34]. Aho et al. showed high zeolite acidity increased reactivity and generated more water and aromatic hydrocarbons [35]. It should be noted that many of these CFP products are not in the EI-MS NIST database, especially those of low oxygen intermediates, and could not be identified (Table S1), whereas we could determine the chemical compositions of all the peaks, thus monitoring the change in the number of oxygens of each molecule.

Table S1 lists all the chemical compositions of cellulose pyrolysis products obtained using Py-GC-dAPCI-TOF MS. The *in situ* CFP is most complex for 1:1 mixture of ZSM-5:cellulose and also listed in the table. They are compared with the corresponding Py-GC-EI-MS data. In cellulose pyrolysis, a total of 82 chemical compositions are determined in Py-GC-dAPCI-TOF MS, in contrast to only 12 that are identified in Py-GC-EI-MS analysis with minimum score of 750 in the NIST database search. Some assignments are ambiguous as the NIST search gives similar scores for several top matching compounds. Twelve additional compounds with lower matching score could be tentatively assigned, labeled as '*', based on the previous reports for their retention times and molecule masses [32]. In case of *in situ* CFP of 1:1 mixture of ZSM-5:cellulose, a total of 137 chemical compositions could be determined in Py-GC-dAPCI-TOF MS whereas only 24 compounds are identified in Py-GC-EI-MS based on NIST search only, and 31 including additional identifications comparing with the literature. Combined altogether without and with catalyst, 142 chemical compositions were determined in Py-GC-dAPCI-TOF MS, compared to only 38 compounds in in-parallel Py-GC-EI-MS analysis that includes both NIST database search result and tentative assignments based on the literature. It should be noted that about thirty and fifty peaks could be seen in chromatograms of Py-GC-EI-MS of cellulose pyrolysis without and with catalyst, respectively (see Fig. 4); however, many of the EI-MS spectra did not match with the NIST database nor literature data.

### 3.3. Semi-quantitative analysis of CFP products with catalyst-to-cellulose load ratio

We have *qualitatively* demonstrated above how the current instrumentation can be utilized for the monitoring of *in situ* CFP process, especially in comparison of different catalysts. To better understand and optimize the CFP process, however, it is necessary to perform

*quantitative* analysis of CFP products. In the current study, *semi-quantitative* analysis was performed by monitoring the relative yields of selected CFP products at catalyst-to-cellulose load ratios of 0, 1, 5, and 10 with ZSM-5. This approach does not allow us to quantitatively compare different molecules because of the difference in ionization efficiencies, but allow us to monitor the quantitative change of each molecule as catalyst load ratio changes.

Fig. 5A shows the relative yields of major cellulose pyrolysis products whose yields decrease as the amount of catalyst load increases. For three most abundant ions (levoglucosan, anhydroglucofuranose, and glycolaldehyde), their yields decrease rapidly as catalyst is added. Their yields are less than 50% of the original amount by adding equal weight amount of catalyst and less than 4% and 1% at catalyst load ratio of 5 and 10, respectively. Three other compounds, 1,4;3,6-dianhydro-α-D-glucopyranose (DAGP), $C_6H_8O_4$ at retention time of 36.6 min (a structural isomer of DAGP), and 5-hydroxymethylfurfural (HMF), decrease a little slow with the equal amount of catalyst, 55~70% of the original amount, but eventually disappear at higher catalyst load ratio. It may suggest that apparent deoxygenation of these compounds is relatively slower initially because they are also catalytically being produced from levoglucosan or anhydroglucofuranose through one or two water loss(es).

Deoxygenation behavior of major low oxygen compounds is shown in Fig. 5B as the change in catalyst load ratio. Their yields increase by adding catalyst, but are eventually disappearing with high amount of catalyst except for $C_3H_6O$ at retention time of 3.1 min and $C_4H_6O$ at 4.3 min whose amounts are not decreasing any further at the catalyst load ratio of 10 compared to those at 5. These low oxygen compounds are most likely produced as partial deoxygenation/cracking of high oxygen compounds as CFP proceeds. Some of them might be further converted to fully deoxygenated compounds via CFP and some others might escape the

reactor without further reaction. Those eventually disappearing at high catalyst load ratio would be the intermediate compounds of full CFP process.

A similar trend was observed by Mukarakate *et al.* in their monitoring of the deactivation of ZSM-5 during *ex situ* CFP of biomass pyrolysis using a molecular beam mass spectrometer (MBMS) [36]. As they passed more pyrolysis vapors through catalytic bed, the amount of fully deoxygenated compounds is decreased, dominated by partially deoxygenated compounds, and eventually dominated by unreacted compounds at high biomass-to-catalyst ratio (or low catalytic load ratio). In their data, intermediate compounds are most abundant when catalytic load ratio is 0.5 to 2, somewhat similar to ours. An important advantage of our approach is that we can trace the trend of individual molecular compounds as the catalyst load ratio changes. Additionally, we can directly determine the chemical compositions of each compound. Their spectrum for intermediate compounds in *ex situ* CFP of cellulose (Fig. S1 of Mukarakate et al. [36]) is extracted from a series of MBMS spectra through principal component analysis and most abundant molecular peaks include *m/z* 82, 96, and 110. By comparing with our data and considering EI-MS produces molecular radical ions ($M^{+\ddot{y}}$), these compounds correspond to $C_5H_6O$ (2-cyclopenten-1-one), $C_5H_4O_2$ (furfural), and $C_6H_6O_2$ (2-propyl furan) shown in Fig. 5B, suggesting good correlation between our and Mukarakate's data despite the differences in instrumentation and experimental conditions.

Completely deoxygenated hydrocarbon compounds, such as the five aromatic hydrocarbons shown in Fig. 5C, follow the opposite trend with major cellulose pyrolysis products shown in Fig. 5A. None of these compounds (or other hydrocarbons) were observed without catalyst. Aromatic hydrocarbons are produced from cracking, dehydration, deoxygenation, and reformation reactions, most notably Diels-Alder reactions, as noted elsewhere [7]. All

hydrocarbons steadily increase in abundance at higher catalyst load. Even at the highest catalyst load ratio of 10, their amounts are increased by 58-78% from those at the load ratio of 5. The high yield of polyaromatic hydrocarbons (PAHs), *e.g.* naphthalene or anthracene, suggests significant coke formation occurs in catalytic fast pyrolysis, which is currently a well-known obstacle in CFP without hydrogen addition. Effective hydrogen to carbon ratio, $(H/C)_{eff}$, is suggested as an important parameter in catalytic fast pyrolysis, defined as (H – 2O)/C with H, C, and O as the moles of hydrogen, carbon, and oxygen, respectively [37]. Cellulose has $(H/C)_{eff}$ of zero, meaning complete dehydration will lead to complete coke or char formation. In fact, the low deoxygenation efficiency at low catalyst load is a result of catalyst deactivation by coke formation [36].

**4. Conclusion**

A critical bottleneck in studying CFP process is the fact that many CFP products cannot be characterized due to significant fragmentations in EI-MS and/or their absence in the database. We developed a new Py-GC-MS approach using dopant-assisted APCI and high-resolution TOF MS analysis. This approach was utilized to efficiently ionize CFP products without or with minimal fragmentations and directly determine their chemical compositions. A total of 142 chemical compositions were identified with this approach for the CFP of cellulose whereas only 38 of them could be identified by in-parallel Py-GC-EI-MS analysis. The utility of our approach was demonstrated to compare catalytic deoxygenation efficiencies of two different catalysts. Furthermore, semi-quantitative analysis was performed to reveal the changes of relative yields of each CFP product as the catalyst-to-biomass load ratio increase.

The current study is limited to semi-quantitative analysis but quantitative analysis would be necessary for the comprehensive understanding of CFP process. For this purpose, we are

currently developing a tandem detection system with flame ionization detector (FID) by splitting the GC capillary outlet between FID and dAPCI-TOF MS. FID signal is proportional to carbon concentration and quantitative in contrast to mass spectrometric ion signals, which have strong dependence on ionization efficiency of each molecule. Once successful, we should be able to obtain both qualitative and quantitative information simultaneously through dAPCI-TOF MS and FID, respectively.

**Acknowledgements**

DPC is partially supported by NSF EpSCOR seed grant.

**Supporting Information**

**Table S1.** Cellulose pyrolysis products observed with and without catalyst (ZSM-5; 1:1 by wt) by Py-GC-APCI-TOF MS and Py-GC-EI-MS.

**Figure Captions.**

**Fig. 1.** A schematic diagram of the Py-GC-dAPCI-TOF MS system used in the study. The inset figure shows the details of the dopant-assisted atmospheric pressure chemical ionization region.

**Fig. 2.** APCI-TOF MS analysis of levoglucosan standard with and without ammonia dopant gas. * represents ammonium and methanol adduct of levoglucosan formed with background gas.

**Fig. 3.** Base peak chromatograms (BPCs) of cellulose pyrolysis analyzed by Py-GC-dAPCI-TOFMS (A) without catalyst, and with (B) ZY and (C) ZSM-5 catalysts. Heteroatom classes are labeled for major peaks.

**Fig. 4.** Py-GC-EI-MS base peak chromatograms (BPCs) of cellulose pyrolysis (A) without catalyst and (B) ZSM-5 catalyst (1:1). *Compounds not identified in NIST database search with a minimum score of 750.

**Fig. 5.** Relative yields of cellulose pyrolysis products as catalyst-to-cellulose load ratio by weight for (A) most abundant compounds in control, (B) partially deoxygenated compounds, and (C) fully deoxygenated compounds. Error bars are standard deviation obtained from three replicates. Abbreviations: DAGP, 1,4;3,6-dianhydro-α-ᴅ-glucopyranose; HMF, 5-hydroxymethylfurfural.

## References


[1] A.V. Bridgwater, *Biomass & Bioenergy*, 38, (2012) 68.

[2] DOE, in, Arlington, VA, 2011.

[3] M.S. Talmadge, R.M. Baldwin, M.J. Biddy, R.L. McCormick, G.T. Beckham, G.A. Ferguson, S. Czernik, K.A. Magrini-Bair, T.D. Foust, P.D. Metelski, C. Hetrick and M.R. Nimlos, *Green Chemistry*, 16, (2014) 407.

[4] M.S. Mettler, A.D. Paulsen, D.G. Vlachos and P.J. Dauenhauer, *Energy & Environmental Science*, 5, (2012) 7864.

[5] M. Ibanez, B. Valle, J. Bilbao, A.G. Gayubo and P. Castano, *Catalysis Today*, 195, (2012) 106.

[6] D.A. Ruddy, J.A. Schaidle, J.R. Ferrell, J. Wang, L. Moens and J.E. Hensley, *Green Chemistry*, 16, (2014) 454.

[7] Y.-T. Cheng and G.W. Huber, *Green Chemistry*, 14, (2012) 3114.

[8] W.-L. Fanchiang and Y.-C. Lin, *Applied Catalysis a-General*, 419, (2012) 102.

[9] D.A. Gunawardena and S.D. Fernando, *Chemical Engineering & Technology*, 34, (2011) 173.

[10] W. Liu, C. Hu, Y. Yang, D. Tong, G. Li and L. Zhu, *Energy Conversion and Management*, 51, (2010) 1025.

[11] B. Valle, A.G. Gayubo, A. Alonso, A.T. Aguayo and J. Bilbao, *Applied Catalysis B-Environmental*, 100, (2010) 318.

[12] A.J. Foster, J. Jae, Y.-T. Cheng, G.W. Huber and R.F. Lobo, *Applied Catalysis a-General*, 423, (2012) 154.

[13] S. Thangalazhy-Gopakumar, S. Adhikari, S.A. Chattanathan and R.B. Gupta, *Bioresource Technology*, 118, (2012) 150.

[14] T. Čajka, J. Hajšlová, R. Kazda and J. Poustka, *Journal of Separation Science*, 28, (2005) 601.

[15] L. Hejazi, D. Ebrahimi, D.B. Hibbert and M. Guilhaus, *Rapid Communications in Mass Spectrometry*, 23, (2009) 2181.

[16] J. Li, J. Cai, T. Yuan, H. Guo and F. Qi, *Rapid Communications in Mass Spectrometry*, 23, (2009) 1269.

[17] Y. Pan, T. Zhang, X. Hong, Y. Zhang, L. Sheng and F. Qi, *Rapid Communications in Mass Spectrometry*, 22, (2008) 1619.

[18] Y. Pan, L. Zhang, T. Zhang, H. Guo, X. Hong and F. Qi, *Journal of Mass Spectrometry*, 43, (2008) 1701.

[19] C. Mukarakate, A.M. Scheer, D.J. Robichaud, M.W. Jarvis, D.E. David, G.B. Ellison, M.R. Nimlos and M.F. Davis, *Review of Scientific Instruments*, 82, (2011) 0331004.

[20] A. Carrasco-Pancorbo, E. Nevedomskaya, T. Arthen-Engeland, T. Zey, G. Zurek, C. Baessmann, A.M. Deelder and O.A. Mayboroda, *Analytical Chemistry*, 81, (2009) 10071.

[21] T. Bristow, M. Harrison and M. Sims, *Rapid Communications in Mass Spectrometry*, 24, (2010) 1673.

[22] R. Garcia-Villalba, T. Pacchiarotta, A. Carrasco-Pancorbo, A. Segura-Carretero, A. Fernandez-Gutierrez, A.M. Deelder and O.A. Mayboroda, *Journal of Chromatography A*, 1218, (2011) 959.

[23] B. Desmazieres, W. Buchmann, P. Terrier and J. Tortajada, *Analytical Chemistry*, 80, (2008) 783.

[24] T. Arthen-Engeland and R. Dunsbach, *Lc Gc Europe*, (2008) 34.
[25] L. Song, D.S. Cho, D. Bhandari, S.C. Gibson, M.E. McNally, R.M. Hoffman and K.D. Cook, *International Journal of Mass Spectrometry*, 303, (2011) 173.
[26] M.a. Amad and S. Sioud, *Rapid Communications in Mass Spectrometry*, 26, (2012) 2517.
[27] J.L. Banyasz, S. Li, J. Lyons-Hart and K.H. Shafer, *Fuel*, 80, (2001) 1757.
[28] A.L. Brown, D.C. Dayton and J.W. Daily, *Energy & Fuels*, 15, (2001) 1286.
[29] J. Huang, C. Liu and S. Wei, *Acta Chimica Sinica*, 67, (2009) 2081.
[30] R. Lanza, D.D. Nogare and P. Canu, *Industrial & Engineering Chemistry Research*, 48, (2009) 1391.
[31] M.S. Mettler, S.H. Mushrif, A.D. Paulsen, A.D. Javadekar, D.G. Vlachos and P.J. Dauenhauer, *Energy & Environmental Science*, 5, (2012) 5414.
[32] P.R. Patwardhan, J.A. Satrio, R.C. Brown and B.H. Shanks, *Journal of Analytical and Applied Pyrolysis*, 86, (2009) 323.
[33] M.S. Mettler, A.D. Paulsen, D.G. Vlachos and P.J. Dauenhauer, *Green Chemistry*, 14, (2012) 1284.
[34] A. Aho, N. Kumar, K. Eränen, T. Salmi, M. Hupa and D.Y. Murzin, *Fuel*, 87, (2008) 2493.
[35] A. Aho, M. Kaldstrom, P. Fardim, N. Kumar, K. Eranen, T. Salmi, B. Holmbon, M. Hupa and D.Y. Murzin, *Cellulose Chemistry and Technology*, 44, (2010) 89.
[36] C. Mukarakate, X. Zhang, A.R. Stanton, D.J. Robichaud, P.N. Ciesielski, K. Malhotra, B.S. Donohoe, E. Gjersing, R.J. Evans, D.S. Heroux, R. Richards, K. Iisa and M.R. Nimlos, *Green Chemistry*, 16, (2014) 1444.
[37] N.Y. Chen, T.F. Degnan and L.R. Koenig, *Chemtech*, 16, (1986) 506.
[38] R. Vinu and L.J. Broadbelt, *Annual Review of Chemical and Biomolecular Engineering, Vol 3*, 3, (2012) 29.

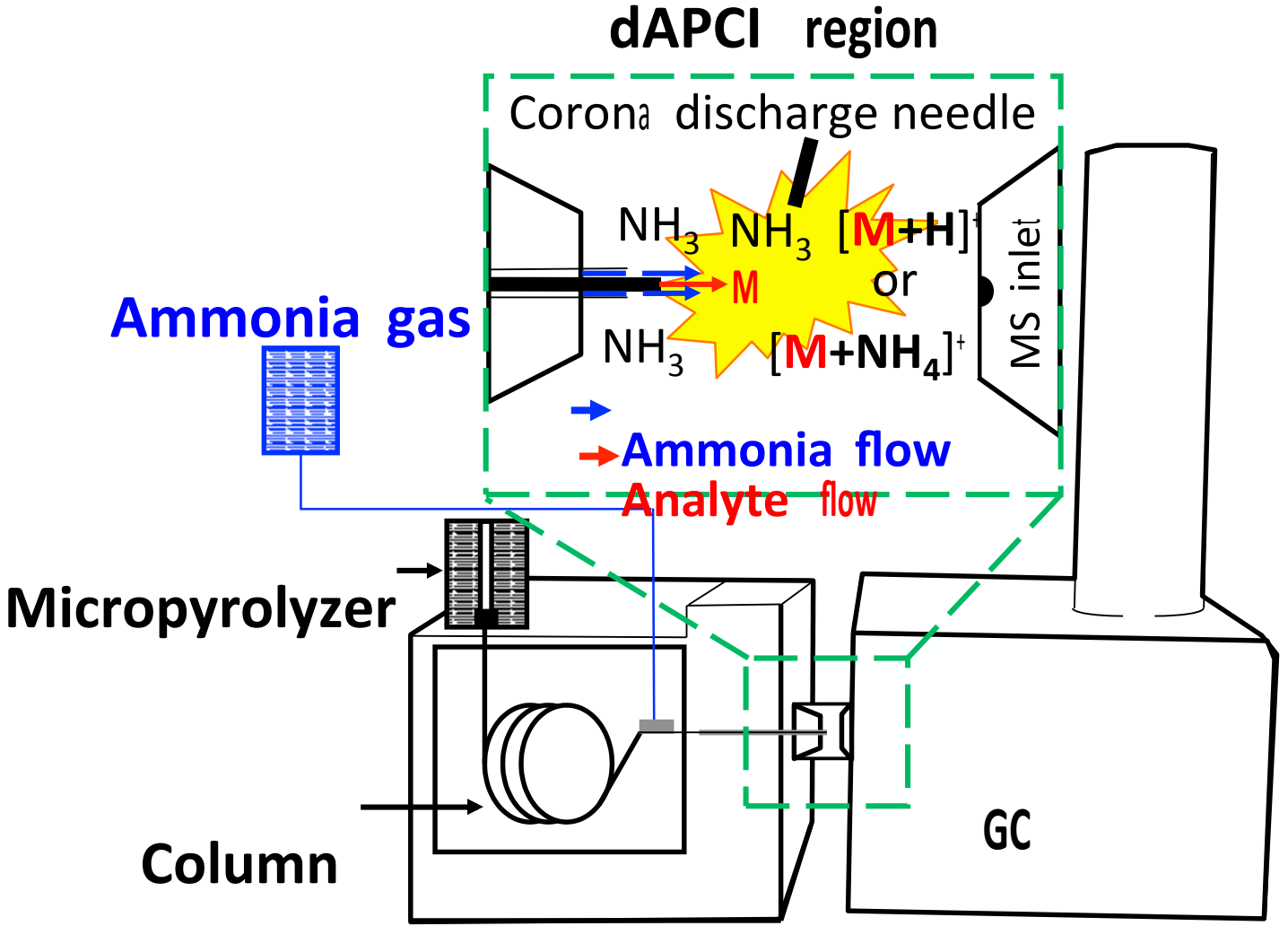
dAPCI region
Corona discharge needle
NH3 NH3 [M+H]+
M or
NH3 [M+NH4]+
MS inlet
Ammonia gas
Ammonia flow
Analyte flow
Micropyrolyzer
Column
GC

# TOF MS

## No Ammonia Gas

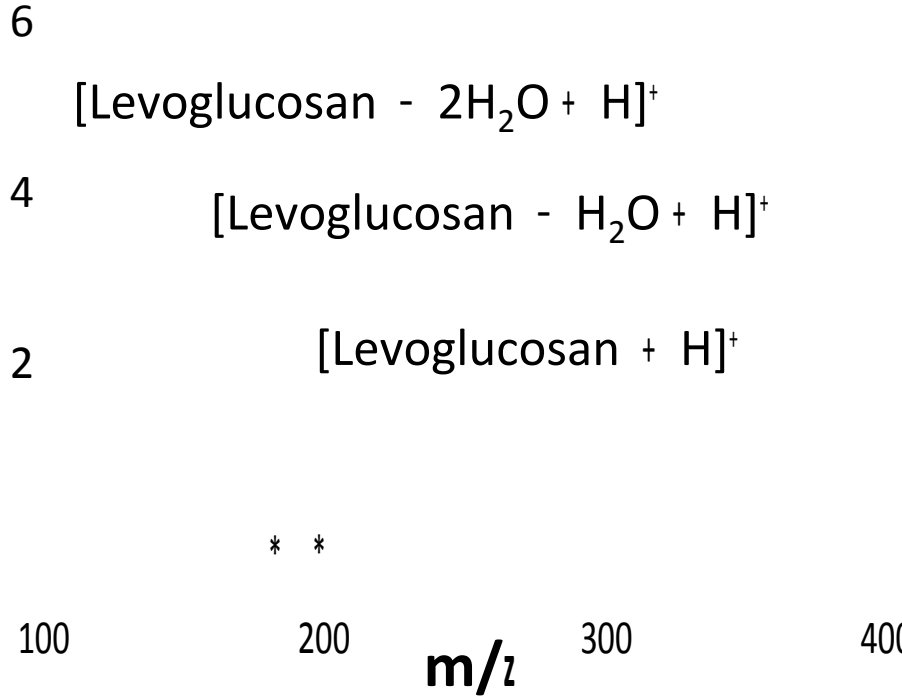


## With Ammonia Gas

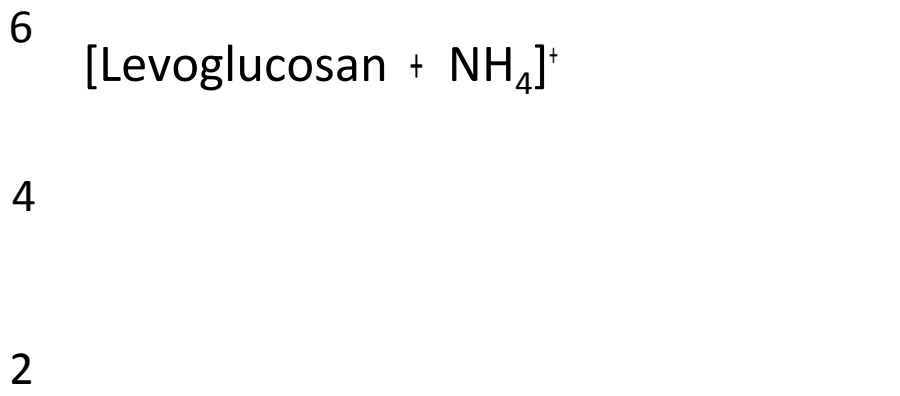

Ion Signal (x10^5)
100
200
m/z
300
400


Ion Signal (x10^5)

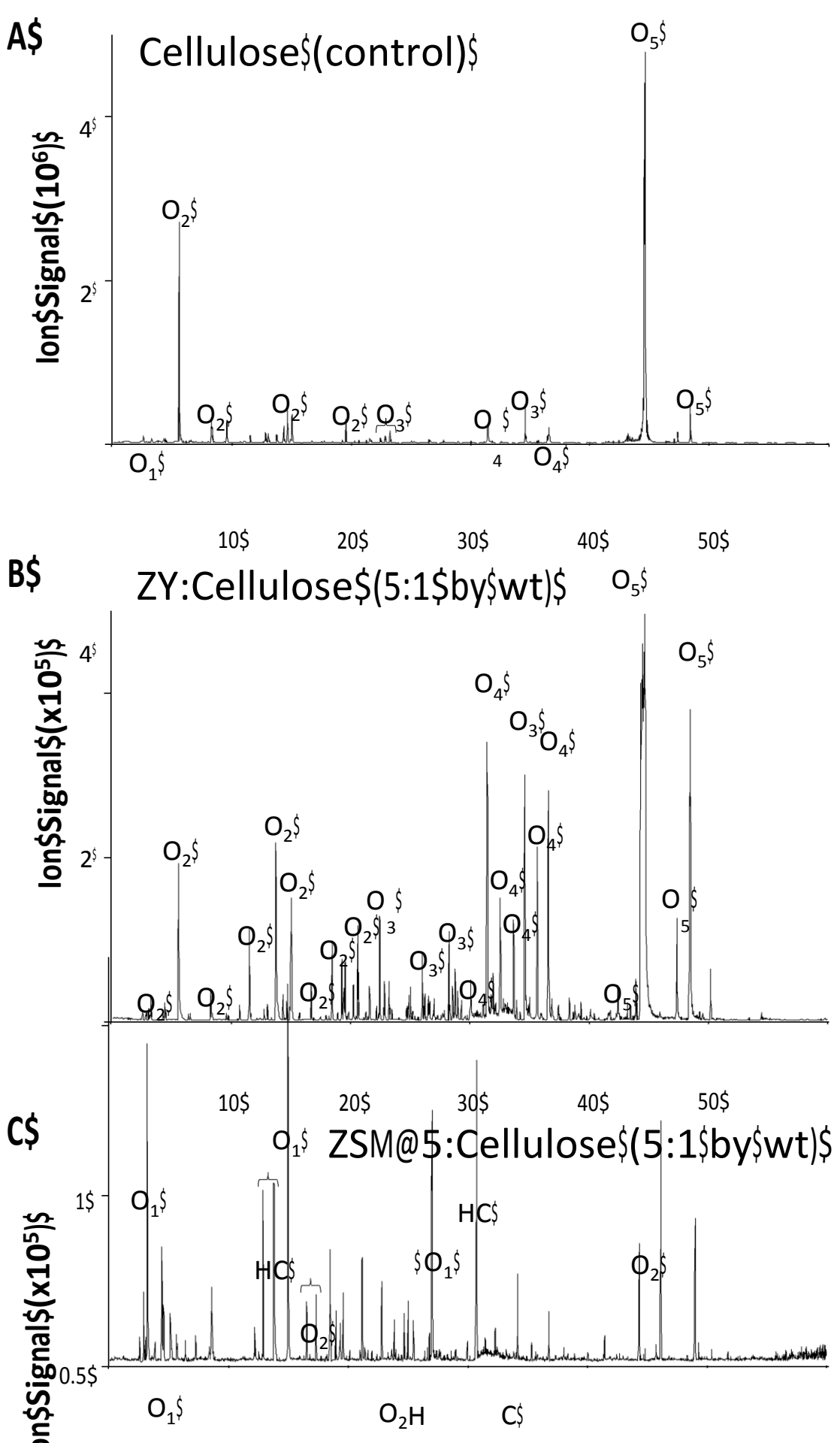
A$
Cellulose$(control)$
Ion$Signal$(10⁶)$
4$
2$
O2$
O1$
O3$
O4$
O5$
10$
20$
30$
40$
50$
B$
ZY:Cellulose$(5:1$by$wt)$
Ion$Signal$(x10⁵)$
4$
2$
O2$
O3$
O4$
O5$
C$
ZSM@5:Cellulose$(5:1$by$wt)$
Ion$Signal$(x10⁵)$
1$
0.5$
O1$
HC$
O2H
C$

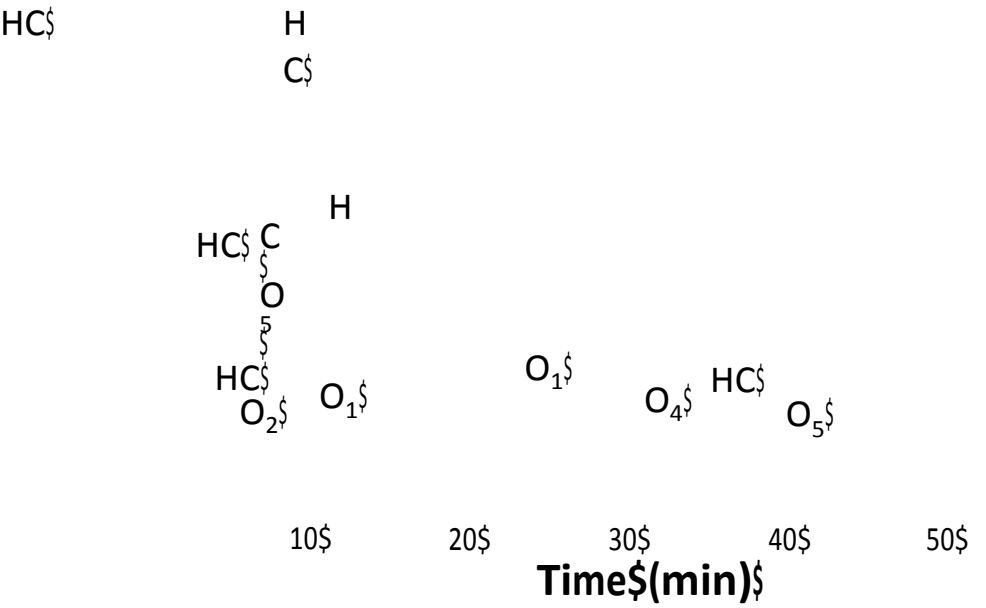
HC$
H
C$
H
HC$
C
$
O
5
$
HC$
O2$
O1$
O1$
O4$
HC$
O5$
10$
20$
30$
40$
50$
Time$(min)$

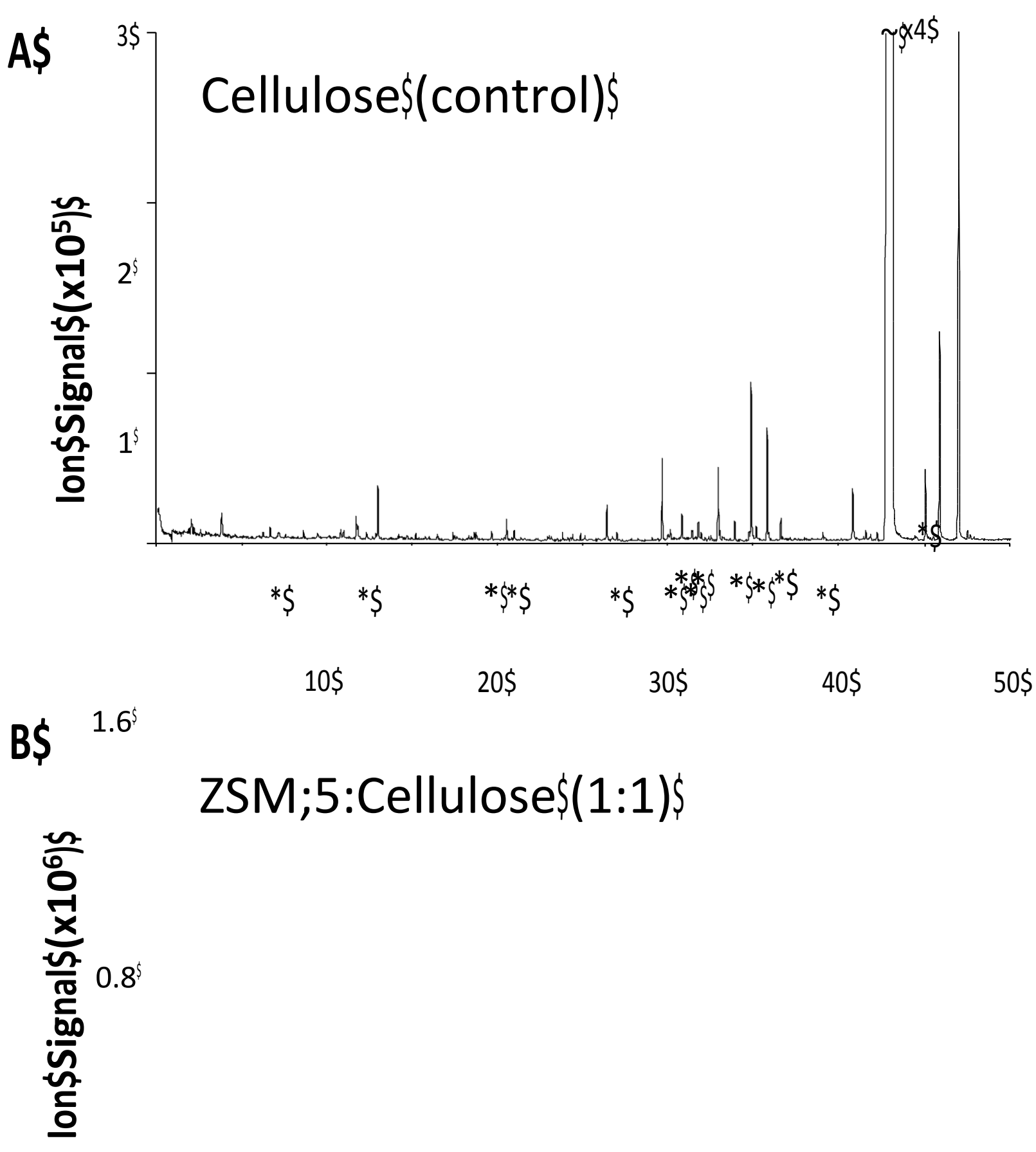
A$
Cellulose$(control)$
Ion$Signal$(x10^5)$
3$
2$
1$
~$x4$
*$
*$
*$
*$*$
*$
*$*$*$
*$*$*$
*$
10$
20$
30$
40$
50$
B$
ZSM;5:Cellulose$(1:1)$
Ion$Signal$(x10^6)$
1.6$
0.8$

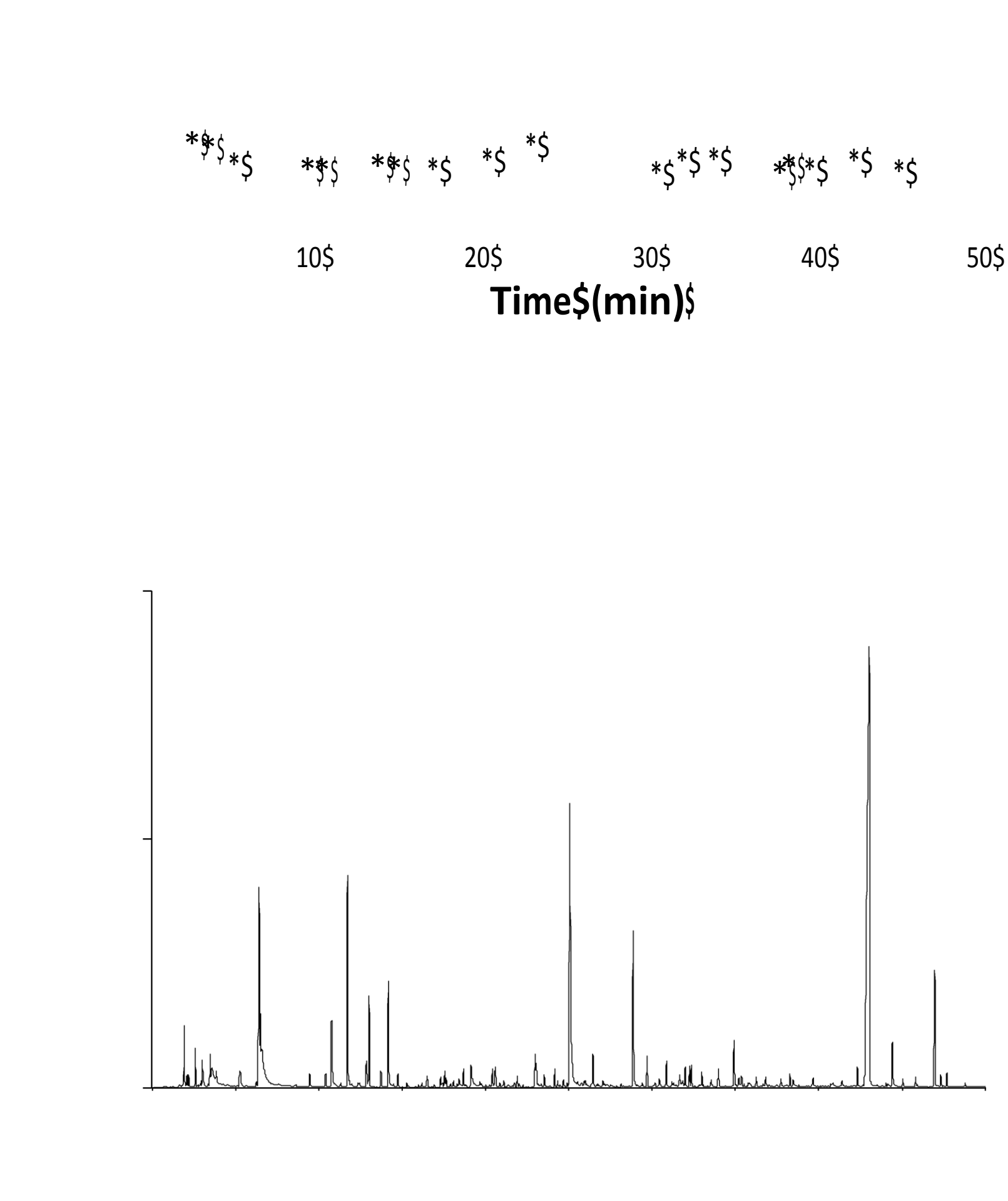
10$
20$
30$
40$
50$
Time$(min)$

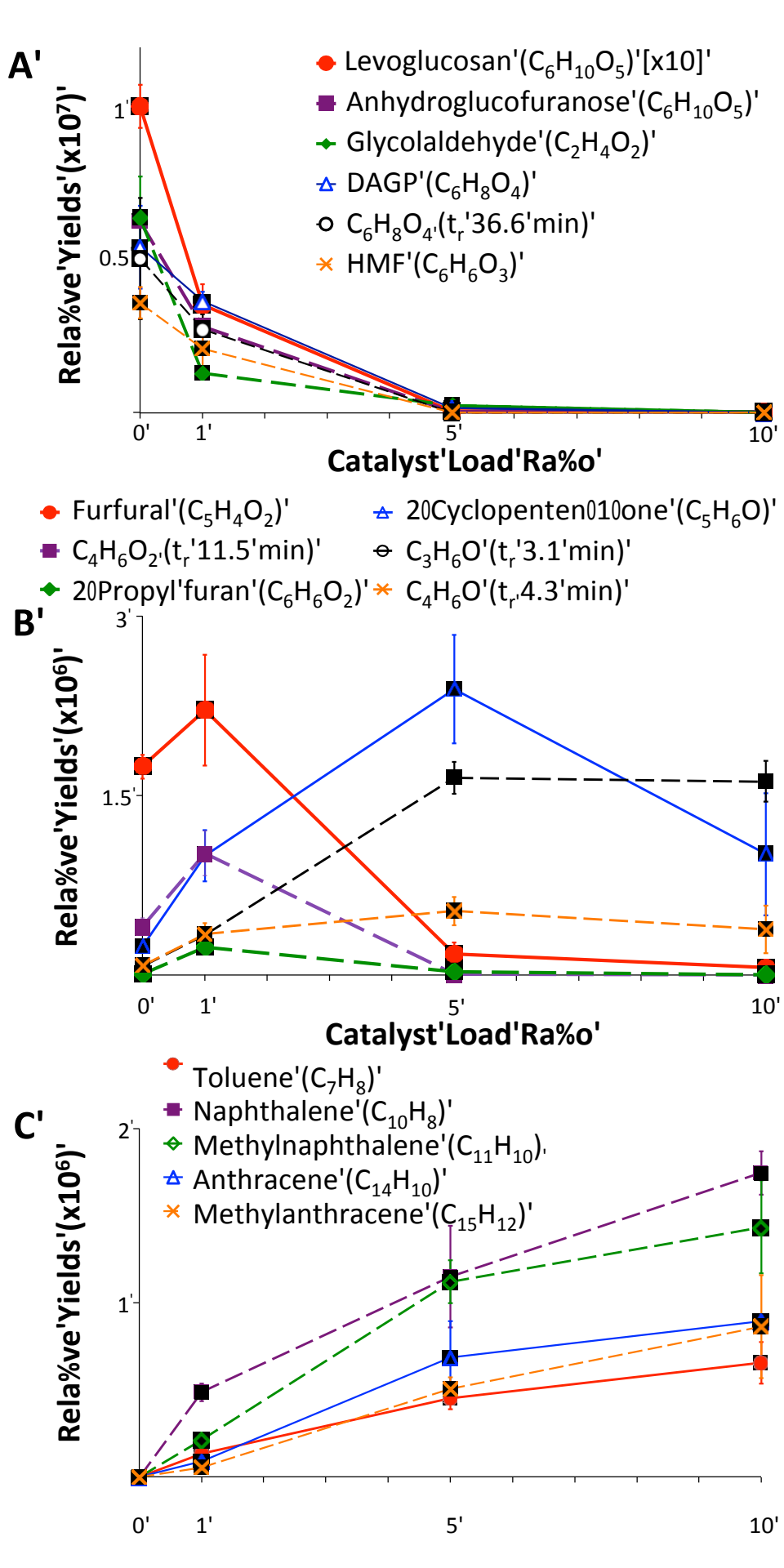
A'
Rela%ve'Yields'(x10⁷)'
1'
0.5
Levoglucosan'(C6H10O5)'[x10]'
Anhydroglucofuranose'(C6H10O5)'
Glycolaldehyde'(C2H4O2)'
DAGP'(C6H8O4)'
C6H8O4'(tr'36.6'min)'
HMF'(C6H6O3)'
0'
1'
5'
10'
Catalyst'Load'Ra%o'
Furfural'(C5H4O2)'
C4H6O2'(tr'11.5'min)'
20Propyl'furan'(C6H6O2)'
20Cyclopenten010one'(C5H6O)'
C3H6O'(tr'3.1'min)'
C4H6O'(tr'4.3'min)'
B'
Rela%ve'Yields'(x10⁶)'
3'
1.5'
0'
1'
5'
10'
Catalyst'Load'Ra%o'
C'
Toluene'(C7H8)'
Naphthalene'(C10H8)'
Methylnaphthalene'(C11H10)'
Anthracene'(C14H10)'
Methylanthracene'(C15H12)'
Rela%ve'Yields'(x10⁶)'
2'
1'
0'
1'
5'
10'

# Catalyst'Load'Ra%o'

**Table S1.** Cellulose pyrolysis products observed with and without catalyst (ZSM-5; 1:1 by wt) by Py-GC-APCI-TOF MS and Py-GC-EI-MS. Identifications for Py-GC-EI-MS data are based on the spectral library search against NIST database with a minimum NIST score of 750. Acronyms: ADGH, 1,5-anhydro-4-deoxy-D-glycero- hex-1-en-3-ulose; DAGP, 1,4;3,6-dianhydro-α-D-glucopyranose; HMF, 5-hydroxymethylfurfural.

*Compounds with matching score less than 750, but tentatively assigned based on cross-reference to previous literature by retention time and molecular ion mass.[1,2]

†Anhydrohexose compounds with score greater than 750 but with exactly same EI-MS spectral pattern to each other and cannot distinguish structural isomers.

| | | PyGC-APCI-TOF MS | | | | | | | PyGC-EI-MS | | |
|---|---|---|---|---|---|---|---|---|---|---|---|
| No. | $t_r$ (min) | m/z experimental | Formula | Adduct | m/z theoretical | Error (ppm) | Control | 1:1 | Assignment | Control | 1:1 |
| 1 | 2.48 | 62.0602 | C2 H4 O | NH4 | 62.0600 | 3.2 | | Y | | | |
| 2 | 2.81 | 68.0261 | C4 H4 O | | 68.0262 | 1.5 | | Y | Furan* | Y | Y |
| 3 | 3.01 | 74.0606 | C3 H4 O | NH4 | 74.0600 | 7.4 | Y | Y | | | |
| 4 | 3.14 | 76.0762 | C3 H6 O | NH4 | 76.0757 | 6.6 | Y | Y | | | |
| 5 | 3.19 | 90.0549 | C3 H4 O2 | NH4 | 90.0550 | 0.8 | Y | Y | Methylglyoxal* | Y | |
| 6 | 3.76 | 82.0415 | C5 H6 O | | 82.0413 | 2.9 | | Y | 2-Methyl furan* | Y | Y |
| 7 | 4.33 | 88.0754 | C4 H6 O | NH4 | 88.0757 | 3.6 | | Y | | | |
| 8 | 4.45 | 104.0697 | C4 H6 O2 | NH4 | 104.0706 | 9.1 | Y | Y | | | |
| 9 | 5.51 | 78.0554 | C2 H4 O2 | NH4 | 78.0550 | 5.7 | Y | Y | Glycolaldehyde* | Y | Y |
| 10 | 6.40 | 88.0757 | C4 H6 O | NH4 | 88.0757 | 0.2 | Y | Y | | | |
| 11 | 6.55 | 88.0757 | C4 H6 O | NH4 | 88.0757 | 0.2 | Y | Y | | | |
| 12 | 6.98 | 116.0695 | C5 H6 O2 | NH4 | 116.0706 | 9.5 | | Y | | | |
| 13 | 7.11 | 78.0554 | C2 H4 O2 | NH4 | 78.0550 | 5.7 | | Y | Acetic acid* | Y | |
| 14 | 7.65 | 118.0852 | C5 H8 O2 | NH4 | 118.0863 | 9.4 | | Y | | | |
| 15 | 8.23 | 92.0702 | C3 H6 O2 | NH4 | 92.0706 | 4.6 | Y | Y | Acetol* | Y | Y |
| 16 | 8.60 | 92.0617 | C7 H8 | | 92.0621 | 4.6 | | Y | Toluene | | Y |
| 17 | 9.55 | 106.0489 | C3 H4 O3 | NH4 | 106.0499 | 9.4 | Y | Y | | | |
| 18 | 9.66 | 100.0752 | C5 H6 O | NH4 | 100.0757 | 5.4 | | Y | | | |
| 19 | 9.73 | 104.0701 | C4 H6 O2 | NH4 | 104.0706 | 5.2 | | Y | | | |

| | | | | | | | | | | | | |
|---|---|---|---|---|---|---|---|---|---|---|---|---|
| 20 | 10.68 | 100.0752 | C5 H6 O | NH4 | 100.0757 | 5.4 | Y | Y | 2-Methylfuran* | Y | | |
| 21 | 11.50 | 104.0701 | C4 H6 O2 | NH4 | 104.0706 | 5.2 | Y | Y | | | | |
| 22 | 12.12 | 102.0542 | C4 H4 O2 | NH4 | 102.0550 | 7.8 | | Y | | | | |
| 23 | 12.38 | 80.0710 | C2 H6 O2 | NH4 | 80.0706 | 4.9 | Y | | | | | |
| 24 | 12.73 | 120.0645 | C4 H6 O3 | NH4 | 120.0655 | 8.1 | Y | Y | | | | |
| 25 | 12.82 | 108.0196 | C6 H4 O2 | | 108.0206 | 8.9 | | Y | | | | |
| 26 | 12.85 | 106.0768 | C8 H10 | | 106.0777 | 8.4 | | Y | p-Xylene | | | Y |
| 27 | 13.03 | 102.0542 | C4 H4 O2 | NH4 | 102.0550 | 7.8 | Y | Y | | | | |
| 28 | 13.37 | 98.0354 | C5 H6 O2 | | 98.0362 | 8.1 | | Y | | | | |
| 29 | 13.77 | 102.0542 | C4 H4 O2 | NH4 | 102.0550 | 7.8 | Y | Y | | | | |
| 30 | 14.00 | 120.0645 | C4 H6 O3 | NH4 | 120.0655 | 8.1 | Y | | | | | |
| 31 | 14.32 | 104.0701 | C4 H6 O2 | NH4 | 104.0706 | 5.2 | Y | Y | | | | |
| 32 | 14.45 | 116.0695 | C5 H6 O2 | NH4 | 116.0706 | 9.5 | | Y | | | | |
| 33 | 14.63 | 120.0645 | C4 H6 O3 | NH4 | 120.0655 | 8.1 | Y | Y | | | | |
| 34 | 14.88 | 100.0752 | C5 H6 O | NH4 | 100.0757 | 5.4 | Y | Y | | | | |
| 35 | 15.00 | 114.0540 | C5 H4 O2 | NH4 | 114.0550 | 8.9 | Y | Y | Furfural | Y | | Y |
| 36 | 15.70 | 128.0694 | C6 H6 O2 | NH4 | 128.0706 | 9.2 | | Y | 2-propyl Furan* | | | Y |
| 37 | 16.49 | 112.0747 | C6 H6 O | NH4 | 112.0757 | 8.5 | | Y | | | | |
| 38 | 16.69 | 116.0697 | C5 H6 O2 | NH4 | 116.0706 | 7.4 | Y | Y | 2-Furanmethanol* | Y | | Y |
| 39 | 16.92 | 116.0697 | C5 H6 O2 | NH4 | 116.0706 | 7.4 | Y | Y | 3-Furanmethanol* | Y | | |
| 40 | 17.27 | 114.0902 | C6 H8 O | NH4 | 114.0913 | 9.7 | | Y | | | | |
| 41 | 17.45 | 118.0855 | C5 H8 O2 | NH4 | 118.0863 | 6.9 | Y | Y | | | | |
| 42 | 17.94 | 128.0694 | C6 H6 O2 | NH4 | 128.0706 | 9.2 | | Y | | | | |
| 43 | 18.19 | 116.0695 | C5 H6 O2 | NH4 | 116.0706 | 9.5 | | Y | | | | |
| 44 | 18.29 | 128.0694 | C6 H6 O2 | NH4 | 128.0706 | 9.2 | | Y | | | | |
| 45 | 18.45 | 114.0540 | C5 H4 O2 | NH4 | 114.0550 | 8.9 | Y | Y | 4-Cyclopentene-1,3-dione | | | Y |
| 46 | 18.90 | 114.0903 | C6 H8 O | NH4 | 114.0913 | 8.8 | | Y | | | | |
| 47 | 19.24 | 99.0433 | C5 H6 O2 | H | 99.0441 | 7.7 | | Y | 2(3H)-Furanone, dihydro-3-methylene- | | | Y |
| 48 | 19.29 | 120.0645 | C4 H6 O3 | NH4 | 120.0655 | 8.1 | Y | Y | | | | |
| 49 | 19.44 | 108.0644 | C3 H6 O3 | NH4 | 108.0655 | 9.7 | Y | Y | | | | |
| 50 | 19.52 | 116.0695 | C5 H6 O2 | NH4 | 116.0706 | 9.1 | Y | Y | | | | |
| 51 | 19.70 | 116.0695 | C5 H6 O2 | NH4 | 116.0706 | 9.1 | | Y | 2-Cyclopenten-1-one, 2-hydroxy- | | | Y |

| | | | | | | | | | | | |
|---|---|---|---|---|---|---|---|---|---|---|---|
| 52 | 19.82 | 127.0381 | C6 H6 O3 | H | 127.0390 | 7.2 | | Y | | | |
| 53 | 20.11 | 102.0542 | C4 H4 O2 | NH4 | 102.0550 | 7.8 | Y | | | | |
| 54 | 20.22 | 116.0697 | C5 H6 O2 | NH4 | 116.0706 | 7.4 | Y | Y | | | |
| 55 | 20.45 | 111.0431 | C6 H6 O2 | H | 111.0441 | 8.9 | | Y | | | |
| 56 | 20.57 | 111.0431 | C6 H6 O2 | H | 111.0441 | 8.9 | Y | Y | 2-Furancarboxaldehyde, 5-methyl- | Y | Y |
| 57 | 20.64 | 132.0644 | C5 H6 O3 | NH4 | 132.0655 | 8.2 | Y | Y | | | |
| 58 | 21.07 | 97.0640 | C6 H8 O | H | 97.0648 | 8.3 | | Y | | | |
| 59 | 21.12 | 116.0611 | C9 H8 | | 116.0621 | 8.3 | | Y | Indene | | Y |
| 60 | 21.27 | 104.0701 | C4 H6 O2 | NH4 | 104.0706 | 5.2 | Y | Y | | | |
| 61 | 21.45 | 128.0694 | C6 H6 O2 | NH4 | 128.0706 | 9.2 | | Y | | | |
| 62 | 21.57 | 102.0543 | C4 H4 O2 | NH4 | 102.0550 | 6.8 | Y | Y | 2(5H)-Furanone* | Y | Y |
| 63 | 21.92 | 111.0431 | C6 H6 O2 | H | 111.0441 | 8.9 | | Y | | | |
| 64 | 22.14 | 116.0697 | C5 H6 O2 | NH4 | 116.0706 | 7.4 | Y | Y | | | |
| 65 | 22.32 | 146.0799 | C6 H8 O3 | NH4 | 146.0812 | 8.6 | Y | Y | | | |
| 66 | 22.44 | 132.0645 | C5 H6 O3 | NH4 | 132.0655 | 7.5 | Y | Y | | | |
| 67 | 22.74 | 114.0540 | C5 H4 O2 | NH4 | 114.0550 | 8.9 | Y | Y | | | |
| 68 | 22.84 | 108.0646 | C3 H6 O3 | NH4 | 108.0655 | 7.9 | Y | Y | | | |
| 69 | 23.22 | 113.0225 | C5 H4 O3 | H | 113.0233 | 7.5 | Y | Y | | | |
| 70 | 23.44 | 144.0644 | C6 H6 O3 | NH4 | 144.0655 | 7.7 | | Y | | | |
| 71 | 24.11 | 128.0694 | C6 H6 O2 | NH4 | 128.0706 | 9.2 | | Y | | | |
| 72 | 24.21 | 128.0694 | C6 H6 O2 | NH4 | 128.0706 | 9.2 | | Y | | | |
| 73 | 24.74 | 104.0698 | C4 H6 O2 | NH4 | 104.0706 | 8.1 | Y | Y | | | |
| 74 | 24.86 | 162.0756 | C6 H8 O4 | NH4 | 162.0761 | 3.0 | | Y | | | |
| 75 | 25.01 | 129.0533 | C6 H8 O3 | H | 129.0546 | 9.8 | Y | Y | | | |
| 76 | 25.19 | 162.0756 | C6 H8 O4 | NH4 | 162.0761 | 3.0 | | Y | | | |
| 77 | 25.22 | 132.0645 | C5 H6 O3 | NH4 | 132.0655 | 7.5 | Y | Y | | | |
| 78 | 25.34 | 162.0756 | C6 H8 O4 | NH4 | 162.0761 | 3.0 | | Y | | | |
| 79 | 25.68 | 146.0799 | C6 H8 O3 | NH4 | 146.0812 | 8.6 | Y | Y | 1,6:2,3-Dianhydro-4-deoxy-β-d-ribo-hexopyranose | Y | |
| 80 | 25.99 | 144.0644 | C6 H6 O3 | NH4 | 144.0655 | 7.7 | Y | Y | | | |
| 81 | 26.14 | 144.0644 | C6 H6 O3 | NH4 | 144.0655 | 7.7 | | Y | | | |
| 82 | 26.22 | 162.0756 | C6 H8 O4 | NH4 | 162.0761 | 3.0 | | Y | | | |
| 83 | 26.26 | 146.0799 | C6 H8 O3 | NH4 | 146.0812 | 8.6 | Y | | | | |

| | | | | | | | | | | | | |
|---|---|---|---|---|---|---|---|---|---|---|---|---|
| 84 | 26.49 | 127.0379 | C6 H6 O3 | H | 127.0390 | 8.7 | Y | Y | | | | |
| 85 | 26.54 | 111.0431 | C6 H6 O2 | H | 111.0441 | 8.9 | | Y | | | | |
| 86 | 26.64 | 120.0643 | C4 H6 O3 | NH4 | 120.0655 | 9.7 | Y | Y | | | | |
| 87 | 26.65 | 134.0799 | C5 H8 O3 | NH4 | 134.0812 | 9.7 | Y | Y | | | | |
| 88 | 26.72 | 148.0595 | C5 H6 O4 | NH4 | 148.0604 | 6.2 | Y | Y | | | | |
| 89 | 26.92 | 128.0609 | C10 H8 | | 128.0621 | 9.2 | | Y | Naphthalene | | | Y |
| 90 | 26.94 | 142.0487 | C6 H4 O3 | NH4 | 142.0499 | 8.1 | Y | | | | | |
| 91 | 27.01 | 162.0756 | C6 H8 O4 | NH4 | 162.0761 | 3.0 | | Y | | | | |
| 92 | 27.16 | 144.0641 | C6 H6 O3 | NH4 | 144.0655 | 9.8 | | Y | | | | |
| 93 | 27.27 | 116.0697 | C5 H6 O2 | NH4 | 116.0706 | 7.4 | Y | Y | | | | |
| 94 | 27.56 | 127.0378 | C6 H6 O3 | H | 127.0390 | 9.5 | | Y | | | | |
| 95 | 27.61 | 128.0694 | C6 H6 O2 | NH4 | 128.0706 | 9.2 | | Y | | | | |
| 96 | 27.74 | 134.0799 | C5 H8 O3 | NH4 | 134.0812 | 9.7 | Y | Y | | | | |
| 97 | 27.86 | 116.0697 | C5 H6 O2 | NH4 | 116.0706 | 7.4 | | Y | | | | |
| 98 | 28.24 | 144.0646 | C6 H6 O3 | NH4 | 144.0655 | 6.3 | Y | Y | Levoglucosenone | | Y | Y |
| 99 | 28.33 | 132.0645 | C5 H6 O3 | NH4 | 132.0655 | 7.5 | | Y | | | | |
| 100 | 28.56 | 150.0754 | C5 H8 O4 | NH4 | 150.0761 | 4.4 | Y | Y | | | | |
| 101 | 28.66 | 134.0802 | C5 H8 O3 | NH4 | 134.0812 | 7.7 | Y | Y | | | | |
| 102 | 28.78 | 150.0754 | C5 H8 O4 | NH4 | 150.0761 | 4.4 | Y | Y | | | | |
| 103 | 28.96 | 143.0330 | C6 H6 O4 | H | 143.0339 | 6.5 | Y | Y | | | | |
| 104 | 29.28 | 162.0772 | C6 H8 O4 | NH4 | 162.0761 | 6.9 | | Y | | | | |
| 105 | 29.64 | 144.0646 | C6 H6 O3 | NH4 | 144.0655 | 6.3 | Y | Y | | | | |
| 106 | 30.09 | 162.0756 | C6 H8 O4 | NH4 | 162.0761 | 3.0 | Y | Y | | | | |
| 107 | 30.59 | 162.0756 | C6 H8 O4 | NH4 | 162.0761 | 3.0 | Y | Y | | | | |
| 108 | 30.69 | 142.0769 | C11 H10 | | 142.0777 | 5.3 | | Y | Methylnaphthalene | | | Y |
| 109 | 31.13 | 162.0756 | C6 H8 O4 | NH4 | 162.0761 | 3.0 | Y | Y | ADGH* | | Y | |
| 110 | 31.43 | 162.0756 | C6 H8 O4 | NH4 | 162.0761 | 3.0 | Y | Y | DAGP | | Y | Y |
| 111 | 31.66 | 132.0645 | C5 H6 O3 | NH4 | 132.0655 | 7.5 | Y | Y | | | | |
| 112 | 31.81 | 162.0756 | C6 H8 O4 | NH4 | 162.0761 | 3.0 | Y | Y | | | | |
| 113 | 31.94 | 162.0756 | C6 H8 O4 | NH4 | 162.0761 | 3.0 | Y | Y | | | | |
| 114 | 32.56 | 162.0756 | C6 H8 O4 | NH4 | 162.0761 | 3.0 | Y | Y | | | | |
| 115 | 33.68 | 162.0756 | C6 H8 O4 | NH4 | 162.0761 | 3.0 | Y | Y | | | | |
| 116 | 33.93 | 162.0756 | C6 H8 O4 | NH4 | 162.0761 | 3.0 | Y | Y | | | | |

| | | | | | | | | | | | | |
|---|---|---|---|---|---|---|---|---|---|---|---|---|
| 117 | 34.15 | 156.0926 | C12 H12 | | 156.0926 | 0.1 | | Y | Dimethylnaphthalene | | | Y |
| 118 | 34.60 | 144.0655 | C6 H6 O3 | NH4 | 144.0655 | 0.0 | Y | Y | HMF | | Y | Y |
| 119 | 34.71 | 162.0756 | C6 H8 O4 | NH4 | 162.0761 | 3.0 | Y | Y | | | | |
| 120 | 34.91 | 134.0802 | C5 H8 O3 | NH4 | 134.0812 | 7.7 | Y | Y | | | | |
| 121 | 35.00 | 144.0649 | C6 H6 O3 | NH4 | 144.0655 | 4.2 | Y | Y | | | | |
| 122 | 35.33 | 154.0766 | C12 H10 | | 154.0777 | 6.9 | | Y | Naphthalene, 2-ethenyl- | | | Y |
| 123 | 35.65 | 162.0756 | C6 H8 O4 | NH4 | 162.0761 | 3.0 | Y | Y | Anhydrohexose† | | Y | |
| 124 | 36.61 | 162.0756 | C6 H8 O4 | NH4 | 162.0761 | 3.0 | Y | Y | Anhydrohexose† | | Y | Y |
| 125 | 36.88 | 180.0868 | C6 H10 O5 | NH4 | 180.0866 | 1.3 | Y | Y | | | | |
| 126 | 37.43 | 150.0754 | C5 H8 O4 | NH4 | 150.0761 | 4.4 | Y | Y | | | | |
| 127 | 38.21 | 149.0587 | C9 H8 O2 | H | 149.0597 | 6.6 | | Y | | | | |
| 128 | 38.36 | 162.0756 | C6 H8 O4 | NH4 | 162.0761 | 3.0 | | Y | | | | |
| 129 | 38.83 | 178.0710 | C6 H8 O5 | NH4 | 178.0710 | 0.0 | Y | Y | | | | |
| 130 | 39.31 | 204.0883 | C8 H10 O5 | NH4 | 204.0866 | 8.4 | | Y | | | | |
| 131 | 42.43 | 180.0870 | C6 H10 O5 | NH4 | 180.0866 | 2.5 | Y | Y | 3,4-Anhydrohexopyranose | | Y | Y |
| 132 | 43.22 | 208.0834 | C7 H10 O6 | NH4 | 208.0816 | 8.6 | | Y | | | | |
| 133 | 43.48 | 208.0834 | C7 H10 O6 | NH4 | 208.0816 | 8.6 | | Y | | | | |
| 134 | 44.38 | 180.0870 | C6 H10 O5 | NH4 | 180.0866 | 2.5 | Y | Y | Levoglucosan | | Y | Y |
| 135 | 46.12 | 179.0849 | C14 H10 | H | 179.0855 | 3.2 | | Y | Anthracene | | | Y |
| 136 | 47.07 | 222.0991 | C8 H12 O6 | NH4 | 222.0972 | 8.7 | Y | Y | | | | |
| 137 | 47.44 | 180.0870 | C6 H10 O5 | NH4 | 180.0866 | 2.5 | Y | Y | Anhydrogalactopyranose | | Y | Y |
| 138 | 48.59 | 180.0870 | C6 H10 O5 | NH4 | 180.0866 | 2.5 | Y | Y | Anhydroglucofuranose | | Y | Y |
| 139 | 48.97 | 193.1017 | C15 H12 | H | 193.1012 | 2.3 | | Y | 9-Methylanthrancene | | | Y |
| 140 | 49.27 | 210.0780 | C10 H8 O4 | NH4 | 210.0761 | 9.3 | | Y | | | | |
| 141 | 49.29 | 193.1017 | C15 H12 | H | 193.1012 | 2.3 | | Y | 2-Methylanthrancene | | | Y |
| 142 | 50.39 | 204.0941 | C16 H12 | | 204.0934 | 3.5 | | Y | Naphthalene, 2-phenyl- | | | Y |


[1] P.R. Patwardhan, J.A. Satrio, R.C. Brown and B.H. Shanks, *Journal of Analytical and Applied Pyrolysis*, 86, (2009) 323.

[2] M.S. Mettler, S.H. Mushrif, A.D. Paulsen, A.D. Javadekar, D.G. Vlachos and P.J. Dauenhauer, *Energy & Environmental Science*, 5, (2012) 5414.